15

Probing Vibrational Energy Relaxation in Proteins Using Normal Modes

Hiroshi Fujisaki, Lintao Bu, and John E. Straub

CONTENTS

15.1 Introduction

The harmonic (or normal mode (NM)) approximation has been a powerful tool for the analysis of few and many-body systems where the essential

BICH: "c472x_c015" — 2005/10/19 — 18:11 — page 301 — #1

dynamics of the system consists of small oscillations about a well-defined mechanically stable structure. The concept of NMs is appealing in science because it provides a simple view for complex systems such as solids and proteins. Though it had been believed that NMs may be too simplistic to analyze the dynamics of proteins, it is by no means always true; the experimental data of neutron scattering for proteins (*B*-factor) indicate that the fluctuations for each residue are well represented by a simplified model using NMs [1]. It was also shown that such a large-amplitude motion as the hinge-bending motion in a protein is well described by a NM [2]. Importantly, NMs have been used to refine the x-ray structures of proteins [3]. Recently, large proteins or even protein complexes can be analyzed by using NMs [4–6].

In this chapter, we are concerned with vibrational energy relaxation (VER) in a protein. This subject is related to our understanding of the functionality of proteins. At the most fundamental level, we must understand the energy flow (pathway) of an injected energy, that is channeled to do useful work. Due to the advance of laser technology, time-resolved spectroscopy can detect such energy flow phenomena experimentally [7]. To interpret experimental data, and to suggest new experiments, theoretical approaches and simulations are essential as they can provide a detailed view of VER. However, VER in large molecules itself is still a challenging problem in molecular science [8]. This is because VER is a typical many-body problem and estimations of quantum effects are difficult [9]. There is a clear need to test and compare the validity of the existing theoretical methods.

We here employ two different methods to estimate the VER rate in a protein, cytochrome c (see Section 15.2 for details). One is the classical equilibrium simulation method [10] with quantum correction factors (QCFs) [11, 12]. The second is the reduced model approach [13], which has been recently employed by Leitner's group [14, 15]. The latter approach is based on NM concepts, which describes VER as energy transfers between NMs mediated by nonlinear resonance [16]. We conclude with a discussion of the validity and applicability of such approaches.

15.2 Cytochrome c

Cytochrome c (cyt c) is one of the most thoroughly physicochemically characterized metalloproteins [17, 18]. It consists of a single polypeptide chain of 104 amino acid residues and is organized into a series of five α-helices and six β-turns. The heme active site in cyt c consists of a 6-coordinate low-spin iron that binds His18 and Met80 as the axial ligands. In addition, two cysteines (Cys14 and Cys17) are covalently bonded through thioether bridges to the heme (see Figure 15.1). Crystal structures of cyt c show that the heme group, which is located in a groove and almost completely buried inside the protein, is nonplanar and somewhat distorted into a saddle-shape geometry.

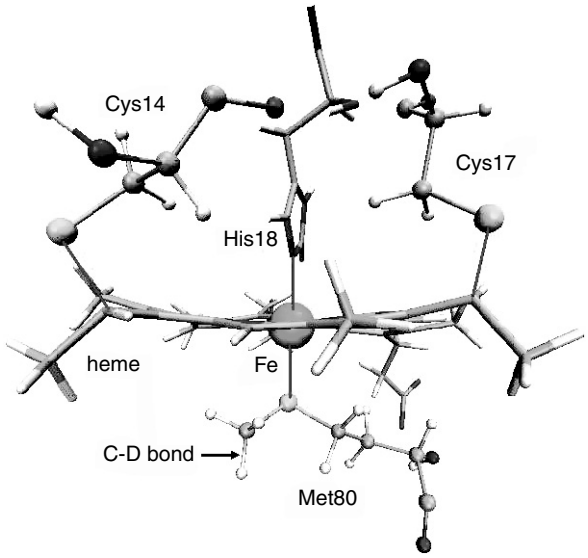

FIGURE 15.1
(See color insert following page 136) The structure of cytochrome c in the vicinity of the heme group, showing the thioether linkages and nonplanar heme geometry.

The reduced protein, ferrocytochrome c (ferrocyt c), is relatively compact and very stable, due to the fact that the heme group is neutral.

The vibrational mode we have chosen for study is the isotopically labeled CD stretch in the terminal methyl group of the residue Met80, which is covalently bonded to Fe in heme (see Figure 15.1). Our simulation model approximates the protein synthesized by Romesberg's group, [19] though their protein contains three deuteriums in Met80 (Met80-3D). The CH and CD stretching bands are located near 3000 and 2200 cm^{-1}, respectively. In contrast with the modeling of photolyzed CO in myoglobin [10], essentially a diatomic molecule in a protein "solvent," we are interested in the relaxation of a selected vibrational mode of a protein. As a result, the modeling is more challenging: There is no clean separation between the system and bath modes because the CD bond is strongly connected to the environment.

15.3 QCF Approach

The classical Landau–Teller–Zwanzig (LTZ) theory of VER is attractive in that it allows us to base our estimate of the VER rate on a classical force autocorrelation function that contains the interaction coupling between the system and bath modes to all orders. The Hamiltonian for such a system is of the Caldeira–Leggett–Zwanzig form, where "bath" coordinates are represented as NMs of

the *bath alone*.[1] The relaxing oscillator is introduced as a local "system" mode, coupled to the bath at all orders, including "bilinear" coupling.

Efforts have been made to introduce quantum effects through the use of "QCFs." The dynamics of the classical system are computed, and the quantum effects are added *a posteriori* in a manner that accounts for the equilibrium quantum statistical distribution of the contributing quantum mechanical degrees of freedom. This approach is summarized below and applied to estimate the rate of VER for the CD bond in the terminal methyl group of Met 80 in cyt c.

15.3.1 Fermi's Golden Rule

Our starting point for computing the rate of VER of the CD stretching mode in cyt c is Fermi's "golden rule" formula. The vibrational population relaxation rate can be written as [13, 20]

$$\frac{1}{T_1} = \frac{\tanh(\beta\hbar\omega_S/2)}{\beta\hbar\omega_S/2}\int_0^\infty dt\cos(\omega_S t)\zeta_{\rm qm}(t) = \frac{\tanh(\beta\hbar\omega_S/2)}{\beta\hbar\omega_S/2}\tilde{\zeta}_{\rm qm}(\omega_S) \tag{15.1}$$

where the force–force correlation function $\zeta_{\rm qm}(t)$ is defined as

$$\zeta_{\rm qm}(t) = \frac{\beta}{2m_S}\langle\mathcal{F}(t)\mathcal{F}(0) + \mathcal{F}(0)\mathcal{F}(t)\rangle_{\rm qm} \tag{15.2}$$

its Fourier transform is $\tilde{\zeta}_{\rm qm}(\omega)$, $\mathcal{F}(t)$ is the quantum mechanical force applied to the system mode considered, m_S is the system (reduced) mass, ω_S is the system frequency, β is an inverse temperature, and the above bracket means a quantum mechanical average. Note that in the classical limit $\hbar \to 0$, the prefactor in front of the integral in Equation (15.1) becomes unity, and the expression reduces to the well-known classical VER formula. The issue is that this limit does not represent well the VER for high frequency modes because of quantum effects (fluctuation), whereas it is difficult to calculate $\zeta_{\rm qm}(t)$.

Rather than using the population relaxation rate $1/T_1$, we could compute the rate of transition between pairs of vibrational quantum states

$$k^{\rm qm}_{n\to n-1} = \frac{2n}{\beta\hbar\omega_S[1+e^{-\beta\hbar\omega_S}]}\tilde{\zeta}_{\rm qm}(\omega) \tag{15.3}$$

where n is the vibrational quantum number. In the limit that $\beta\hbar\omega_S \gg 1$ as we consider here, the splitting between vibrational levels is large compared with

[1] As shown below, the *classical* LTZ formula can be considered as a classical limit of the quantum mechanical population relaxation rate $1/T_1$. This result is derived by using *both* Fermi's golden rule and Bader–Berne theory [20]. Though the transition rate $k_{n\to n-1}$ itself can be derived without any assumption on the bath Hamiltonian, the Bader–Berne result stems from the assumption that the bath Hamiltonian is an ensemble of harmonic oscillators.

the thermal energy. At equilibrium, the system oscillator will be ground state dominated, and we find that

$$\frac{1}{T_1} \simeq \frac{2\tilde{\zeta}_{\rm qm}(\omega_S)}{\beta \omega_S} \simeq k_{1\to 0}^{\rm qm} \tag{15.4}$$

For such a system, we are free to consider the rate of vibrational relaxation in terms of the ensemble averaged relaxation rate $1/T_1$ or the microscopic rate constant $k_{1\to 0}^{\rm qm}$ — the results will be equivalent.

In the limit that $\beta \omega_S \to 0$, on the other hand, the splitting between states becomes much smaller than the thermal energy and the results are *not* equivalent. The rate constant $k_{1\to 0}^{qm}$ diverges, while the population relaxation rate $1/T_1$ is well behaved

$$\frac{1}{T_1} \simeq \tilde{\zeta}_{\rm qm}(\omega_S) \tag{15.5}$$

In this chapter, we will present our results in terms of $1/T_1$.

15.3.2 Quantum Correction Factor

While $\zeta_{\rm qm}(t)$ is difficult to compute for all but the simplest systems, it is often possible to compute the classical analog

$$\zeta_{\rm cl}(t) = \frac{\beta}{m_S}\langle \mathcal{F}(t)\mathcal{F}(0)\rangle_{\rm cl} \tag{15.6}$$

for highly nonlinear systems consisting of thousands of atoms. The above bracket denotes a classical ensemble average. The challenge is to relate the quantum mechanical correlation function to its classical analog. An approach explored by Skinner et al. has proved to be quite productive [12]. It involves relating the spectral density of the quantum system to that of the analogous classical system as

$$\tilde{\zeta}_{\rm qm}(\omega_S) = Q(\omega_S)\tilde{\zeta}_{\rm cl}(\omega_S) \tag{15.7}$$

where $Q(\omega_S)$ is referred to as the "QCF." The QCF must obey detailed balance $Q(\omega) = Q(-\omega)e^{\beta\ \omega}$ and satisfy the "classical" limit that as $\beta\omega$ becomes small, the QCF approaches unity. Using this result, we may rewrite Equation (15.1) as

$$\frac{1}{T_1^{\rm QCF}} \simeq \frac{Q(\omega_S)}{\beta \omega_S}\tilde{\zeta}_{\rm cl}(\omega_S) \tag{15.8}$$

Note that the classical VER rate is defined as $1/T_1^{\rm cl} \equiv \tilde{\zeta}_{\rm cl}(\omega_S)$.

The QCF for a one phonon relaxation mechanism is

$$Q_{\rm H}(\omega) = \frac{\beta \omega}{1 - e^{-\beta\ \omega}} \tag{15.9}$$

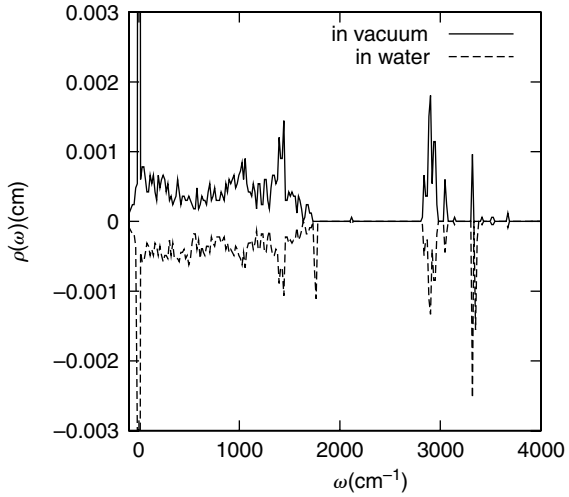

FIGURE 15.2
Density of states $\rho(\omega)$ for cyt c in vacuum (solid line) and in water (dashed line) at 300 K calculated by INM analysis.

However, as the CD stretching mode falls in the transparent region of the DOS (Figure 15.2), a 1:1 Fermi resonance (linear resonance) is not the possible mechanism of VER. As such, the lowest order mechanism available for the VER of the CD mode should involve two phonons.

We have employed Skinner's QCF approach for two-phonon relaxation [12]. If the two-phonon mechanism assumes that two lower frequency bath modes, having frequencies ω_A and $\omega_S - \omega_A$, are each excited by one quantum of vibrational energy, the appropriate QCF is

$$Q_{\mathrm{HH}}(\omega_S) = Q_{\mathrm{H}}(\omega_A) Q_{\mathrm{H}}(\omega_S - \omega_A) \tag{15.10}$$

Alternatively, if the assumed two-phonon mechanism is one that leads to the excitation of one bath vibrational mode of frequency ω_A, with the remaining energy $\square(\omega_S - \omega_A)$ being transferred to lower frequency bath rotational and translational modes, the appropriate QCF is

$$Q_{\mathrm{H\text{–}HS}}(\omega_S) = Q_{\mathrm{H}}(\omega_A)\sqrt{Q_{\mathrm{H}}(\omega_S - \omega_A)}\mathrm{e}^{\beta\ (\omega_S - \omega_A)/4} \tag{15.11}$$

The functions Q_{H}, Q_{HH}, $Q_{\mathrm{H\text{–}HS}}$ are called the harmonic, harmonic–harmonic, and harmonic–harmonic–Schofield QCF, respectively.

15.3.3 NM Calculations for Cyt c

To compute the QCF requires a knowledge of, or guess at, the mechanism of VER. Likely bath modes must be identified and a combination

of those modes must meet a resonance condition enforced by the conservation of energy in the transition. The candidate modes are identified using quenched normal mode (QNM) or instantaneous normal mode (INM) calculations.

In Figure 15.2, we show the density of states (DOS) for cyt c in vacuum and in water at 300 K. These are the INM spectra, so they contain some negative (actually imaginary) components. The basic structure of this DOS is similar to that of other proteins such as myoglobin [10, 16]. The librational and torsional motions are embedded in lower frequency regions below 2000 cm^{-1}, and vibrational motions are located in higher frequency regions around 3000 cm^{-1}. There is a transparent region between 2000 and 3000 cm^{-1}; the peak due to the CD mode falls in this region near 2200 cm^{-1}. The VER of this CD mode is our target in this study. Note, furthermore, that the spectra in vacuum and in water are very similar. This indicates that water solvent might not affect the simulation results. This conjecture will be confirmed below.

15.3.4 Application to VER of the CD Bond in Cyt c

Bu and Straub [11] employed the QCF approach to estimate the VER rate of a CD bond in the terminal methyl group of Met80 in cyt c (Figure 15.1). Their calculations were done using the program Chemistry at HARvard Mechanics (CHARMM) [21], and cyt c was surrounded by water molecules at 300 K. In this work, we have used molecular dynamics simulations of cyt c *in vacuum* at 300 K to compute the classical autocorrelation function for the force acting on the same CD bond. The results have been used to make estimates of both $1/T_1^{\mathrm{cl}}$ and $1/T_1^{\mathrm{QCF}}$.

In Figure 15.3, the force autocorrelation function and its power spectrum are shown for four different trajectories. We have observed that the force fluctuation and the magnitude of the power spectrum for cyt c in vacuum is very similar to those computed for cyt c in water. We conclude that the effects of water on the VER rate are negligible. With the CD bond frequency $\omega_S = 2133\ \mathrm{cm}^{-1}$, we find $1/T_1^{\mathrm{cl}} = \tilde{\zeta}_{\mathrm{cl}}(\omega_S) \simeq 1\ \mathrm{psec}^{-1}$, that is, the classical VER time is about 1 psec.

To apply QCFs for two-phonon relaxation, Equations (15.10) and (15.11) to this situation, we need to know ω_A. We have found that the CD mode is strongly resonant with two lower frequency modes, 1655th (685.48 cm^{-1}) and 3823rd (1443.54 cm^{-1}) modes because $|\omega_S - \omega_{1655} - \omega_{3823}| = 0.03\ \mathrm{cm}^{-1}$. We might be able to choose $\omega_A = 1443.54$ or 685.48 cm^{-1}.

In Figure 15.4, we show the ω_A dependence of the normalized QCF, that is, $\tilde{Q} = Q/(\beta\hbar\omega_S) = T_1^{\mathrm{cl}}/T_1^{\mathrm{QCF}}$ at 300 K and at 15 K. If we choose $\omega_A = 1443.54\ \mathrm{cm}^{-1}$ at 300 K, $\tilde{Q} = 2.3$ for the harmonic–harmonic QCF and 2.8 for the H–HS QCF. Thus, we have $T_1^{\mathrm{QCF}} = T_1^{\mathrm{cl}}/\tilde{Q} = 0.3 \sim 0.4$ psec. It is interesting to note $\tilde{Q}$ at 15 K varies significantly depending on the QCF employed. We will discuss this feature in Sec. 15.4.4.

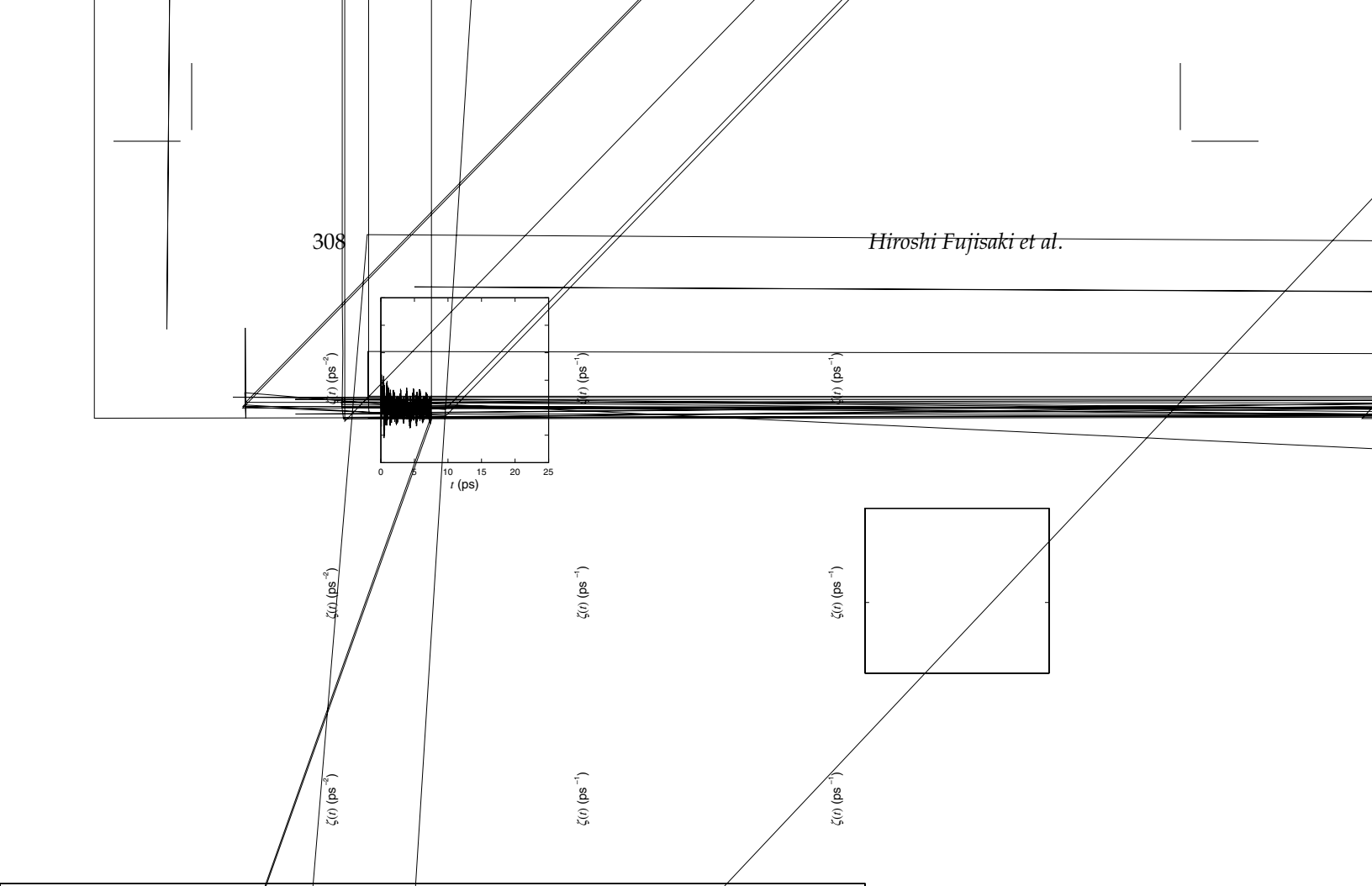

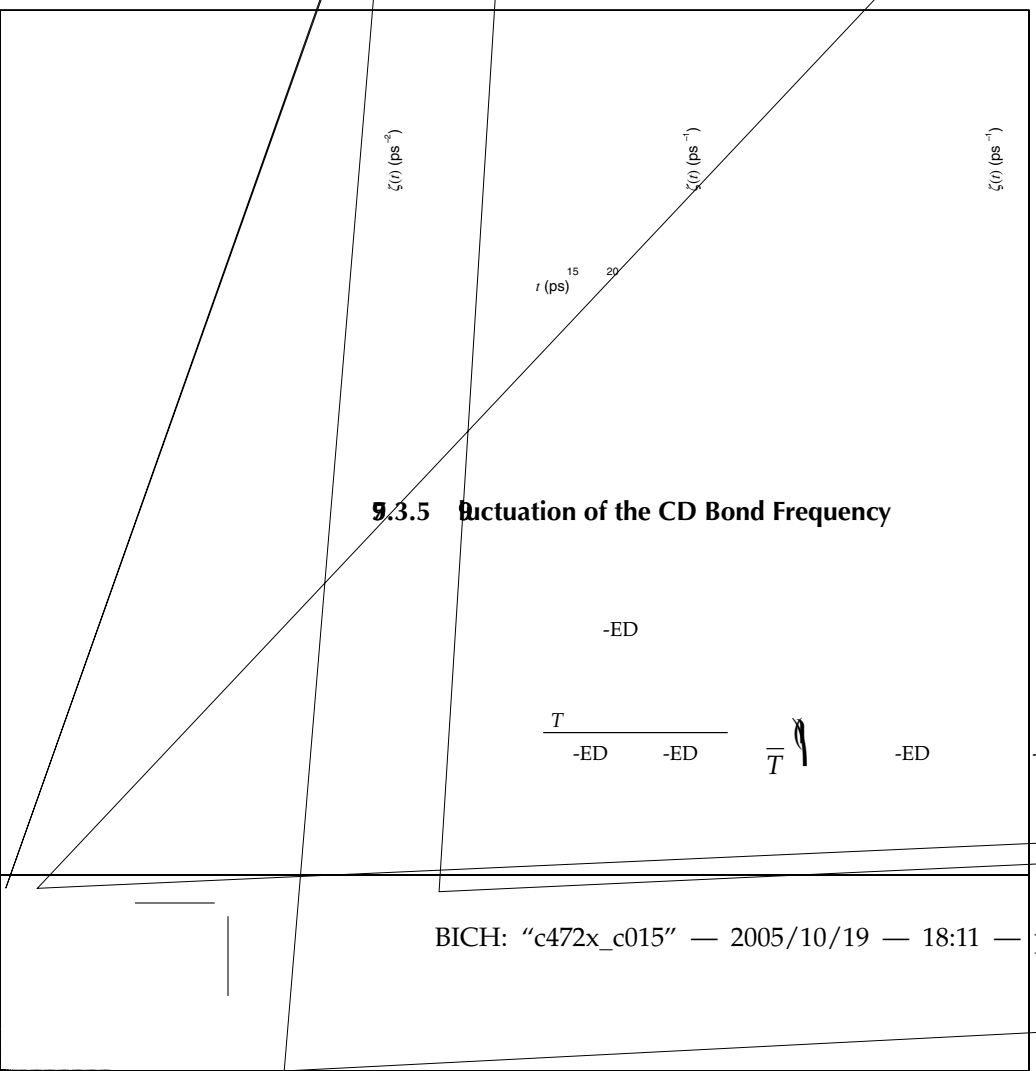

9.3.5 Fluctuation of the CD Bond Frequency

-ED

$\frac{T}{\text{-ED}\quad\text{-ED}}$ $\overline{T}$ ¶ -ED -ED

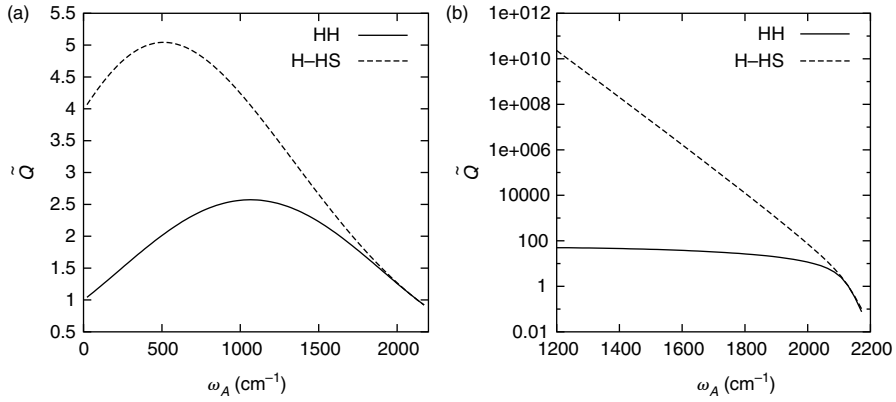

FIGURE 15.4
Normalized HH and H–HS QCF at 300 K (a) and at 15 K (b) as a function of the bath mode frequency ω_A.

where the overline means a long time (T) average, and $\delta\omega_{\mathrm{CD}}(t) = \omega_{\mathrm{CD}}(t) - \overline{\omega_{\mathrm{CD}}(t)}$. The correlation time is defined as

$$\tau_c = \frac{1}{(\Delta\omega)^2}\int_0^\infty C(t)dt \tag{15.13}$$

where $(\Delta\omega)^2 = C(0)$. From Figure 15.5, we found $\Delta\omega \simeq 8.5$ cm^{-1} and $\tau_c \simeq 0.2$ psec. Since $\Delta\omega\tau_c \ll 1$, according to Kubo's analysis [22], the line

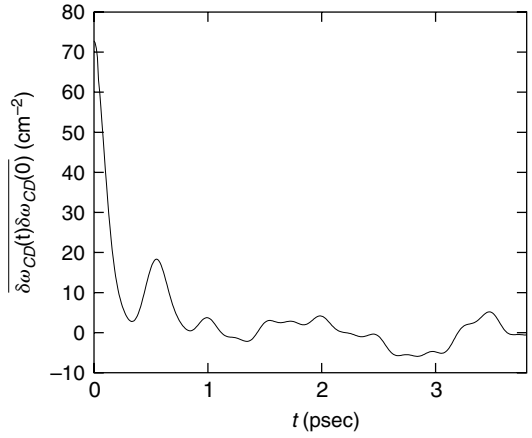

FIGURE 15.5
The frequency autocorrelation function calculated from the instantaneous normal mode analysis. The data up to 20 psec were used to calculate the correlation function.

the system and bath modes are uncoupled and noninteracting. The interaction "coupling" between the system and bath modes first appears at third order. In this section, we describe a perturbation theory estimate of the rate of VER of the CD mode that represents the system–bath coupling to lowest, third order in the system and bath coordinates.

15.4.1 Reduced Model for a Protein

The reduced model approach utilizes the NM picture of a protein, expanding the residual term perturbatively as [23]

$$\mathcal{H} = \mathcal{H}_S + \mathcal{H}_B + \mathcal{V}_3 + \mathcal{V}_4 + \cdots \tag{15.14}$$

$$\mathcal{H}_S = \frac{p_S^2}{2} + \frac{\omega_S^2}{2} q_S^2 \tag{15.15}$$

$$\mathcal{H}_B = \sum_k \frac{p_k^2}{2} + \frac{\omega_k^2}{2} q_k^2 \tag{15.16}$$

$$\mathcal{V}_3 = \sum_{k,l,m} G_{klm} q_k q_l q_m \tag{15.17}$$

$$\mathcal{V}_4 = \sum_{k,l,m,n} H_{klmn} q_k q_l q_m q_n \tag{15.18}$$

Thus the force applied to the system mode is

$$\mathcal{F} = -\frac{\partial \mathcal{V}}{\partial q_S} = -3 \sum_{k,l} G_{S,k,l} q_k q_l - 4 \sum_{k,l,m} H_{S,k,l,m} q_k q_l q_m + \cdots \tag{15.19}$$

where we have used the permutation symmetry of G_{klm} and H_{klmn}. If it is enough to include the lowest order terms proportional to G_{klm}, substituting them into Fermi's golden rule Equation (15.1), we can derive an approximate VER rate as [13]

$$\frac{1}{T_1} \simeq \frac{1}{m_S \omega_S} \frac{1 - \mathrm{e}^{-\beta \omega_S}}{1 + \mathrm{e}^{-\beta \omega_S}} \sum_{k,l} \left[\frac{\gamma \zeta_{k,l}^{(+)}}{\gamma^2 + (\omega_k + \omega_l - \omega_S)^2} + \frac{\gamma \zeta_{k,l}^{(+)}}{\gamma^2 + (\omega_k + \omega_l + \omega_S)^2} + \frac{\gamma \zeta_{k,l}^{(-)}}{\gamma^2 + (\omega_k - \omega_l - \omega_S)^2} + \frac{\gamma \zeta_{k,l}^{(-)}}{\gamma^2 + (\omega_k - \omega_l + \omega_S)^2} \right] \tag{15.20}$$

where we have included a width parameter γ to broaden a delta function, and defined the following:

$$\zeta_{k,l}^{(+)} = \frac{\hbar^2}{2} \frac{(A_{k,l}^{(2)})^2}{\omega_k \omega_l} (1 + n_k + n_l + 2 n_k n_l) \tag{15.21}$$

$$\zeta_{k,l}^{(-)} = \frac{\hbar^2}{2} \frac{(A_{k,l}^{(2)})^2}{\omega_k \omega_l} (n_k + n_l + 2 n_k n_l) \tag{15.22}$$

$$A_{k,l}^{(2)} = -3 G_{S,k,l} \tag{15.23}$$

$$n_k = 1/(e^{\beta \hbar \omega_k} - 1) \tag{15.24}$$

15.4.2 Maradudin–Fein Formula

There exists another well-known formula to describe the VER rate, the Maradudin–Fein (MF) formula [24, 14],

$$W = W_{\mathrm{decay}} + W_{\mathrm{coll}} \tag{15.25}$$

$$W_{\mathrm{decay}} = \frac{\hbar}{2 m_S \omega_S} \sum_{k,l} \frac{(A_{k,l}^{(2)})^2}{\omega_k \omega_l} (1 + n_k + n_l) \frac{\gamma}{\gamma^2 + (\omega_S - \omega_k - \omega_l)^2} \tag{15.26}$$

$$W_{\mathrm{coll}} = \frac{\hbar}{m_S \omega_S} \sum_{k,l} \frac{(A_{k,l}^{(2)})^2}{\omega_k \omega_l} (n_k - n_l) \frac{\gamma}{\gamma^2 + (\omega_S + \omega_k - \omega_l)^2} \tag{15.27}$$

with a width parameter γ. Note that Equations (15.20) and (15.25) are equivalent in the limit of $\gamma \to 0$ as shown by Kenkre et al. [25]. However, they disagree with a finite width parameter such as $\gamma \sim 100\ \mathrm{cm}^{-1}$. In this chapter,

we use the MF formula and consider its classical limit ($\hbar \to 0$) defined as

$$W^{\mathrm{cl}}_{\mathrm{decay}} = \frac{1}{2m_S\beta\omega_S} \sum_{k,l} \frac{(A^{(2)}_{k,l})^2}{\omega_k\omega_l} \left(\frac{1}{\omega_k} + \frac{1}{\omega_l}\right) \frac{\gamma}{\gamma^2 + (\omega_S - \omega_k - \omega_l)^2} \tag{15.28}$$

$$W^{\mathrm{cl}}_{\mathrm{coll}} = \frac{1}{m_S\beta\omega_S} \sum_{k,l} \frac{(A^{(2)}_{k,l})^2}{\omega_k\omega_l} \left(\frac{1}{\omega_k} - \frac{1}{\omega_l}\right) \frac{\gamma}{\gamma^2 + (\omega_S + \omega_k - \omega_l)^2} \tag{15.29}$$

We note some properties of the formula: $W_{\mathrm{decay}} \geq W^{\mathrm{cl}}_{\mathrm{decay}}$ and $W_{\mathrm{coll}} \leq W^{\mathrm{cl}}_{\mathrm{coll}}$, which is derived from

$$\frac{1/(e^x - 1) + 1/(e^y - 1)}{1/x + 1/y} \geq 1 \tag{15.30}$$

$$\frac{1/(e^x - 1) - 1/(e^y - 1)}{1/x - 1/y} \leq 1 \tag{15.31}$$

for $x, y > 0$. We can define an effective QCF as

$$Q_{\mathrm{eff}} = \frac{W}{W^{\mathrm{cl}}} = \frac{W_{\mathrm{decay}} + W_{\mathrm{coll}}}{W^{\mathrm{cl}}_{\mathrm{decay}} + W^{\mathrm{cl}}_{\mathrm{coll}}} \tag{15.32}$$

This should be compared with the normalized QCFs [$\tilde{Q} = Q(\omega_S)/(\beta\hbar\omega_S)$] found in the literature.

15.4.3 Third-Order Coupling Elements

To apply the MF theory to the case of CD bond relaxation in cyt c, we must numerically compute the third-order coupling elements. As the protein has more than 10^3 modes, there are more than 10^6 third-order coupling elements representing the coupling of the "system" CD bond to the "bath" modes of the surrounding protein and solvent.

We have employed the finite difference approximation

$$A^{(2)}_{mn} = -\frac{1}{2} \frac{\partial^3 V}{\partial q_S \partial q_m \partial q_n} \simeq -\frac{1}{2} \sum_{ij} U_{im} U_{jn} \frac{K_{ij}(\Delta q_S) - K_{ij}(-\Delta q_S)}{2\Delta q_S} \tag{15.33}$$

where U_{ik} is an orthogonal matrix that diagonalizes the (mass-weighted) Hessian matrix at the mechanically stable structure K_{ij}, and $K_{ij}(\pm\Delta q_S)$ is a Hessian matrix calculated at a shifted structure along the direction of a selected mode with a shift $\pm\Delta q_S$.

Note that, in the large number of coupling elements, most are small in magnitude. Of those that are larger, most fail to meet the resonance condition

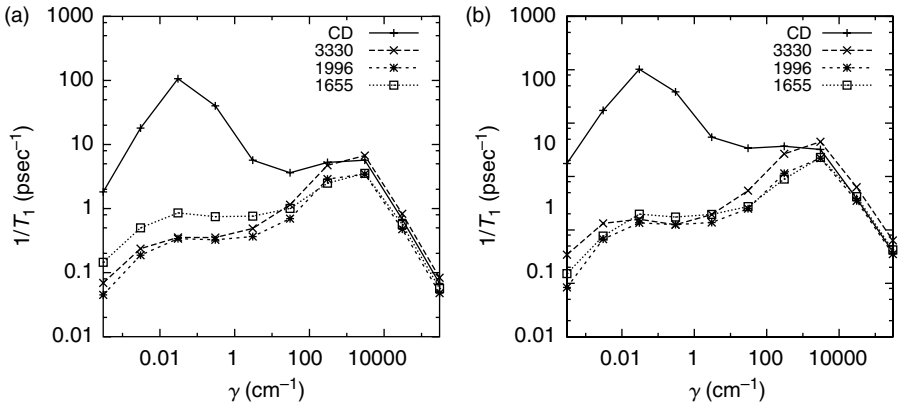

FIGURE 15.6
VER rates for the CD mode ($\omega_{CD} = 2129.1\ cm^{-1}$) and the other lower frequency modes ($\omega_{3330} = 1330.9\ cm^{-1}$, $\omega_{1996} = 829.9\ cm^{-1}$, $\omega_{1655} = 685.5\ cm^{-1}$) as a function of γ at 300 K (a) and at 15 K (b).

and do not contribute significantly to the perturbative estimate of the VER rate (see Reference 13 for the details).

15.4.4 Width Parameter

We show the width parameter γ dependence of the VER rate in Figure 15.6.[2] We consider other lower frequency modes ($\omega_{3330} = 1330.9\ cm^{-1}$, $\omega_{1996} = 829.9\ cm^{-1}$, and $\omega_{1655} = 685.5\ cm^{-1}$) as well as the CD mode ($\omega_{CD} = 2129.1\ cm^{-1}$) for comparison. From the former analysis of the frequency autocorrelation function Equation (15.12), we might be able to take $\gamma \simeq \Delta\omega \sim 3\ cm^{-1}$ for the CD mode, and we have $T_1 \simeq 0.2$ psec, which agrees with the previous result with QCFs: $T_1^{QCF} = 0.3 \sim 0.4$ psec.

We also see that the lower frequency modes have longer VER time, a few psec, which agrees with the calculations by Leitner's group employing the MF formula [15]. The main contribution to the VER rate at $\gamma = 3\ cm^{-1}$ comes from 1655th mode ($685.5\ cm^{-1}$), a heme torsion, and the 3823rd ($1443.5\ cm^{-1}$) mode, an angle bend in Met80 (∼20%). Interestingly, we can conceive a peak around $\gamma = 0.03\ cm^{-1}$. Given this width parameter, the contribution from the two modes is more than 90%. We can say that 1655th and 3823rd modes are resonant with the CD mode because they satisfy the resonant condition ($|\omega_{1655} + \omega_{3823} - \omega_{CD}| \simeq 0.03\ cm^{-1}$) and the coupling elements between them is relatively large ($|A^{(2)}_{1655,3823}| \simeq 5.1$ kcal/mol/Å^3).

This close resonance does not necessarily lead to the conclusion that it forms the dominant channel for VER of the CD stretch. There is a competing

[2]Note two limiting cases of γ dependence: $1/T_1 \propto \gamma$ when γ is very small, and $1/T_1 \propto 1/\gamma$ when γ is very large. This is easily recognized from the Lorentzian form.

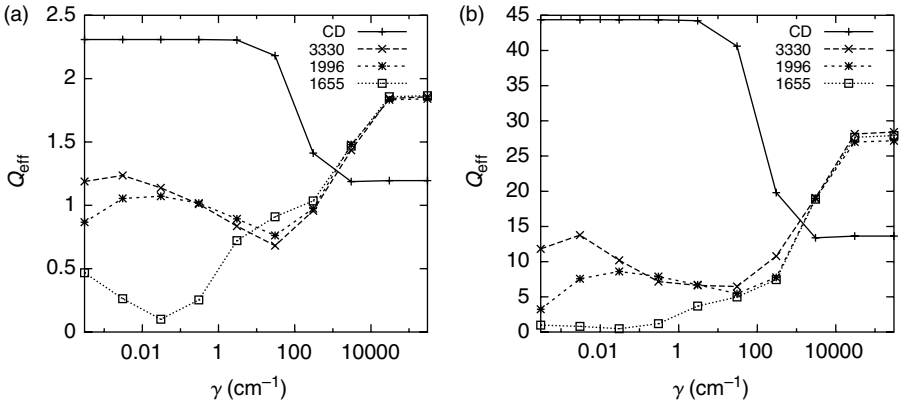

FIGURE 15.7
Effective QCF for the CD mode ($\omega_{\rm CD} = 2129.1$ cm^{-1}) and the other lower frequency modes ($\omega_{3330} = 1330.9$ cm^{-1}, $\omega_{1996} = 829.9$ cm^{-1}, $\omega_{1655} = 685.5$ cm^{-1}) as a function of γ at 300 K (a) and at 15 K (b).

near-resonance involving the 3330th mode (1330.9 cm^{-1}), an angle bending mode of Met80, and the 1996th mode (829.9 cm^{-1}), a stretch-bend mode in Met80. While the resonance is not close (it is within 31.7 cm^{-1}), the coupling element is quite large ($|A^{(2)}_{3330,1996}| \simeq 22.3$ kcal/mol/Å^3). With a larger value of $\gamma = 30$ cm^{-1}, this combination of bath modes becomes the dominant channel for VER of the CD stretch. Clearly, the uncertainty in our force field, used to compute the vibrational frequencies, and the value of γ, which is rather poorly defined, prevents us from concluding that one or another of these two channels will dominate VER of the CD stretch at room temperature.

In Figure 15.7(a), we show the effective QCF calculated from Equation (15.32) at 300 K, which is $Q_{\rm eff} \simeq 2.3$ for the CD mode with $\gamma = 3$ cm^{-1}. This value better agrees with the (normalized) HH QCF [Equation (15.10)], compared to the H–HS QCF [Equation (15.11)]. The $Q_{\rm eff}$ for the other modes are more or less unity, which indicates that these modes behave classically at 300 K.[3] In contrast, as is shown in Figure 15.7(b), $Q_{\rm eff}$ at 15 K is very large ($Q_{\rm eff} \simeq 40$), which implies that the classical VER rate becomes small because it is proportional to the temperature (see also Figure 15.8). A similar trend is found in the right of Figure 15.4, where the HH QCF ($\tilde{Q} \simeq 40$) is comparable to $Q_{\rm eff}$. On the other hand, the H–HS QCF gives an exponentially large value of $\tilde{Q}$, showing strong deviations from $Q_{\rm eff}$. We should bear in mind that different QCFs lead to significantly different conclusions at low temperatures.

[3]We notice an interesting behavior for 1655th mode, that is, $Q_{\rm eff}$ becomes very much smaller than unity at $\gamma \simeq 0.03$ cm^{-1}. In this case, we observe that $W_{\rm coll} \gg W_{\rm decay}$ because of the resonance: $\omega_{1655} + \omega_{3823} - \omega_{\rm CD} \simeq 0$ (actually 0.03 cm^{-1}). In such a case, $Q_{\rm eff}$ becomes less than unity because $W_{\rm coll} \leq W^{\rm cl}_{\rm coll}$.

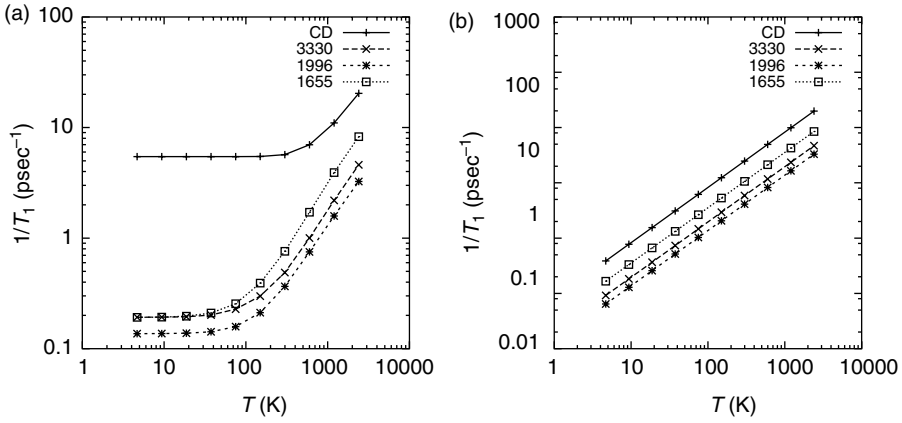

FIGURE 15.8
Quantum (a) and classical (b) VER rates for the CD mode ($\omega_{CD} = 2129.1$ cm^{-1}) and the other lower frequency modes ($\omega_{3330} = 1330.9$ cm^{-1}, $\omega_{1996} = 829.9$ cm^{-1}, $\omega_{1655} = 685.5$ cm^{-1}) as a function of temperature with $\gamma = 3$ cm^{-1}.

15.4.5 Temperature Dependence

In Figure 15.8, we show the temperature dependence of the quantum and classical VER rate calculated by the MF formula and the classical limit of the MF formula. At high temperatures (∼1000 K), the quantum VER rate agrees with the classical one, but they deviate at low temperatures. The former becomes constant due to the remaining quantum fluctuation (zero point energy) whereas the latter decreases as $\propto$ (temperature). The "cross over temperature" where the VER behaves classically is smaller for the lower frequency modes compared to that of the CD mode as expected.

15.5 Discussion

15.5.1 Comparison with Experiment

Here we compare our results with the experiment by Romeberg's group [19]. They measured the shifts and widths of the spectra for different forms of cyt c; the widths of the spectra full width at half maximum (FWHM) were found to be $\Delta\omega_{FWHM} \simeq 6.0 \sim 13.0$ cm^{-1}. From the discussions of Section 15.3.5, we can theoretically neglect inhomogeneous effects, and estimate the VER rate simply as

$$T_1 \sim 5.3/\Delta\omega_{FWHM} \text{ (psec)} \tag{15.34}$$

which corresponds to $T_1 \simeq 0.4 \sim 0.9$ psec. This estimate is similar to the QCF prediction using Equation (15.8) (0.3 ∼ 0.4 psec) and the reduced model approach using Equations (15.20) or (15.25) (0.2 ∼ 0.3 psec). We note

that this value should be compared to the VER time of the C–H stretch in N-methylacetamide-D [$CH_3(CO)ND(CH_3)$] [26], which is also sub psec. Further experimental studies, for example, on temperature dependence of absorption spectra or on time-resolved spectroscopy, will clarify the methodology that is more applicable.

Romesberg's group studied Met80-3D (methionine with three deuteriums), while we have examined Met80-1D (methionine with one deuterium). In the case of Met80-3D, there are three peaks in the transparent region. It should be possible to consider the VER of each of the three modes, to make a more direct comparison of the predictions of our theoretical models with the results of their experimental studies.

15.5.2 Validity of Fermi's Golden Rule

We next discuss the validity of our approaches. Since our starting point is the perturbative Fermi's golden rule, our two approaches should have a limited range of validity. Naively speaking, the force applied on the CD mode should be small enough, but how small should it be?

We follow Kubo's derivation of a quantum master equation using the projection operator technique [22]. He derived an equation for the evolution of the system density operator $\sigma(t)$

$$\frac{\partial}{\partial t}\sigma(t) = -\frac{1}{\square^2}\int_{-\infty}^{t} d\tau [q(t)q(\tau)\sigma(\tau)\Phi(t-\tau) - q(t)\sigma(\tau)q(\tau)\Phi(-t+\tau) + \sigma(\tau)q(\tau)q(t)\Phi(-t+\tau) - q(\tau)\sigma(\tau)q(t)\Phi(t-\tau)] \tag{15.35}$$

The interaction Hamiltonian is assumed to be $\mathcal{H}_{\rm int} = -q\mathcal{F}$, as in our case, that is, q is the system coordinate and $\mathcal{F}$ contains the bath coordinates. We have defined the force autocorrelation function $\Phi(t) = {\rm Tr}_B\{\rho_B\mathcal{F}(t)\mathcal{F}(0)\} = \langle\mathcal{F}(t)\mathcal{F}(0)\rangle$. Note that Equation (15.35) is just a von Neumann equation using the projection operator technique, and it is not a master equation yet.

If $\Phi(t)$ decays fast, we can replace $\sigma(\tau)$ in the integral with $\sigma(t)$, and the dynamics becomes an approximate Markovian dynamics. If this approximation is valid, Fermi's golden rule describes the relaxation dynamics of $\sigma(t)$ [22]. The validity of the golden rule relies on the validity of the Markov approximation.

From Equation (15.35), the relaxation rate of $\sigma(t)$ can be estimated as

$$1/\tau_r \sim (\langle q^2\rangle\mathcal{F}^2/\square^2)\tau_c \tag{15.36}$$

where we have assumed

$$\Phi(t) \simeq \mathcal{F}^2 e^{-|t|/\tau_c} \tag{15.37}$$

The Markov approximation [$\sigma(\tau) \simeq \sigma(t)$] holds for

$$\tau_r \gg \tau_c \tag{15.38}$$

TABLE 15.1

The Parameters in Equation (15.39) for Various Molecules in AKMA Units (Unit Length = 1 Å, Unit Time = 0.04888 psec, Unit Energy = 1 kcal/mol).

	$\langle q^2 \rangle$	$\mathcal{F}^2$	τ_c	ϵ
CD in cyt c	0.01	5.0	1.0	0.5
HOD in D_2O	0.01	5.0	1.0	0.5
CN^- in water	0.002	1.0	0.5	0.01
CO in Mb	0.002	1.0	1.0	0.02

Source: The data for HOD in D_2O is taken from R. Rey and J.T. Hynes, *J. Chem. Phys.* 104, 2356 (1996); for CN^- in water from R. Rey and J.T. Hynes, *J. Chem. Phys.* 108, 142 (1998); for CO in Mb from D.E. Sagnella and J.E. Straub *Biophys. J.* 77, 70 (1999).

We have a criterion for the validity of the Markov approximation

$$\epsilon \equiv \langle q^2 \rangle \mathcal{F}^2 \tau_c^2 / \square^2 \ll 1 \tag{15.39}$$

In our case as well as the case of HOD in D_2O, the ratio is "just" small (see Table 15.1). Applying Fermi's golden rule to these situations should be regarded as a reasonable estimate of the VER rate. As alternative approaches that avoid this underlying Markov approximation, one can employ more "advanced" methods as mentioned in Section 15.6.

15.5.3 Higher-Order Coupling Terms

So far, we have only included the third-order coupling terms to describe the VER of the CD mode. However, we must be concerned with the relative contribution of higher-order mechanism, for example, the contribution due to the fourth-order coupling terms in Equation (15.18). This is a very difficult question. As there are many terms ($\sim 10^9$) included, we cannot directly calculate all of them for cyt c. We have found that it is not sufficient to include only the third-order coupling terms to reproduce the fluctuation of the force on the CD bond. However, this does not necessarily mean that the VER rate calculated from the third-order coupling terms is inadequate.

The main contribution from the fourth-order coupling terms to the VER rate and the force fluctuation are written as

$$\Delta \left(\frac{1}{T_1} \right) \sim \sum_{k,l,m} \frac{|H_{S,k,l,m}|^2}{\omega_k \omega_l \omega_m} \delta(\omega_S - \omega_k - \omega_l - \omega_m) \tag{15.40}$$

and

$$\Delta \langle \delta \mathcal{F}^2 \rangle \sim \sum_{k,l,m} \frac{|H_{S,k,l,m}|^2}{\omega_k \omega_l \omega_m} \tag{15.41}$$

respectively. Even if $\Delta\langle\delta\mathcal{F}^2\rangle$ becomes large, $\Delta(1/T_1)$ is not necessarily large because of the resonance condition ($\omega_S - \omega_k - \omega_l - \omega_m \simeq 0$). It is a future task how to evaluate the effects due to higher-order coupling terms. It might be interesting to compare the classical limit using the reduced model approach and the LTZ approach because there is no ambiguity about how to choose QCFs [29].

15.6 Summary

In this chapter, we have examined VER in a protein from the QCF approach and the reduced model approach, and compared the results. For the CD mode in cyt c (in vacuum) at room temperature, both approaches yield similar results for the VER rate, which is also similar to an estimate based on an experiment by Romesberg's group. Our work demonstrates both the feasibility and accuracy of a number of theoretical approaches to estimate VER rates of selected modes in proteins.

The QCF approach is appealing in that the calculation of the force autocorrelation function is straightforward and feasible, even for systems of thousands of degrees of freedom. Moreover, the classical force autocorrelation function includes all orders of nonlinearity in the interaction between the system oscillator and the surrounding bath. A weakness of the QCF approach is that we do not know which QCF to choose *a priori*. We must assume a mechanism for VER before computing the rate. Moreover, the temperature dependence of the rate of VER is sensitive to the mechanism, whether it involves few phonons or many phonons. The choice of the form of the QCF can make a significant difference in the predicted rate of VER at lower temperatures.

On the other hand, the reduced model approach is appealing in that the quantum dynamics of the reduced system is accurately treated. Using the reduced model approach, there are two ways to estimate the quantum mechanical force autocorrelation function: (1) numerical calculation of the quantum dynamics for a model Hamiltonian of a few degrees of freedom, including all orders of nonlinearity in the potential and (2) analytical solution for the quantum dynamics using perturbation theory that includes many bath modes but only the lowest-order nonlinear coupling between the system and bath modes. We have employed the latter approach through the use of the MF formula. A weakness of our reduced model approach is that the method neglects the higher-order coupling elements beyond third order, which cannot be justified *a priori* [30, 31].

We have pursued a comparative study in which we seek *consensus* in the estimates of $1/T_1$ the results of the QCF approach and the perturbation theory. A rather remarkable result of our study is that while the absolute value of the quantum corrections to the classical VER theory are large (on the order of

a factor of 40), the results of the QCF and the perturbation theory approaches are in close agreement. This is all the more remarkable given the fact that the results of the perturbation theory require a calculation of the third-order coupling constants and the estimation of the "lifetime" parameter γ. As we have shown, the dominant channel for VER, derived from the perturbation theory, depends upon the choice of γ. For smaller $\gamma = 3\ \text{cm}^{-1}$, the dominant mechanism is a close resonance (within 0.1 cm^{-1}), a combination of a heme torsion and Met80 angle bending mode, with a weak coupling. For larger $\gamma = 30\ \text{cm}^{-1}$, the dominant mechanism appears to be a less perfect resonance (within 31.7 cm^{-1}), a combination of a different angle bending mode and a bend-stretch mode in Met 80, with a strong coupling. Such detailed knowledge of γ is essential to predict a mechanism for VER.

Our study raises two important questions. (1) What is the optimal set of coordinates for modeling and interpreting VER in proteins? In the QCF approach, we treated the relaxing bond (CD bond) as a *local mode* that is coupled to vibrational modes of the bath. In the reduced model approach, on the other hand, we treated all the vibrational modes including the relaxing mode (CD mode) as *NMs* that are coupled to each other with the third-order nonlinear coupling terms. Our numerical results showed that the two approaches give similar results for the VER rate of the CD bond or mode, but it remains to be seen that this is a kind of coincidence or there is a theoretical ground of their equivalence (if the QCF is appropriately chosen) (2) What is the physical origin of the width parameter γ and how to calculate it? In this study, we suggested to use the relation $\gamma \simeq \Delta\omega$ where $\Delta\omega$ represents the fluctuation of the CD mode (or bond) frequency. We think this is reasonable but there is few theoretical explanation to this. If the VER rate does not significantly depend on γ, this is not a serious problem, but this is not always the case. Thus we need an "ab initio" way to derive the width parameter γ. One appealing way is to regard γ as a hopping rate between potential basins (inherent structures) [32, 33]. Recent advances may provide a theoretical underpinning for the direct calculation of the "lifetime" width parameters [34].

The results of our study are derived through the use of an approximate empirical energy function (force field), which has not been "tuned" to provide accurate frequencies of vibration for all protein modes. Our predicted rates of VER depend sensitively on the closeness of the resonance between the system and bath modes. Clearly, we must resort to the reparameterization of the empirical potential to fit with experimental data or higher levels of theory (ab initio quantum chemistry calculation) in an effort to refine our estimates of the frequencies of vibration and the details of nonlinear coupling between vibrational modes of the protein. This is a challenge for both experimental and theoretical studies.

Recent advances in experiment and theory make the present time an exciting one for the detailed study of protein dynamics. A variety of methods have been applied to examine VER in molecules, including nonequilibrium MD methods [35], time-dependent self-consistent field methods [31, 36],

mixed quantum–classical methods [37], and semiclassical methods [38, 39]. In addition, it is now possible to compute spectroscopic observables such as absorption spectra or 2D-IR signals [40, 41] as probes of protein structures and dynamics. Extensions of these studies will provide us with an increasingly detailed picture of the dynamics of proteins and its relation to structures and functions.

Acknowledgments

We thank Prof. S. Takada, Prof. T. Komatsuzaki, Prof. Y. Mizutani, Prof. K. Tominaga, Prof. S. Okazaki, Prof. F. Romesberg, Prof. J.L. Skinner, Prof. D.M. Leitner, Prof. I. Ohmine, Prof. S. Saito, Prof. R. Akiyama, Prof. K. Takatsuka, Dr. H. Ushiyama, Dr. T. Miyadera, Dr. S. Fuchigami, Dr. T. Yamashita, Dr. Y. Sugita, Dr. M. Ceremeens, Dr. J. Zimmerman, and Dr. P.H. Nguyen for helpful comments and discussions, and Prof. S. Mukamel and Prof. Y. Tanimura for informing the references related to nonlinear spectroscopy. We thank the National Science Foundation (CHE-0316551) for its generous support to our research.

References

1. N. Go, T. Noguchi, and T. Nishikawa, "Dynamics of a small protein in terms of low-frequency vibrational modes," *Proc. Natl Acad. Sci. USA* **80**, 3696 (1983); B. Brooks and M. Karplus, "Harmonic dynamics of proteins: normal modes and fluctuations in bovine pancreatic trypsin inhibitor," *Proc. Natl Acad. Sci. USA* **80**, 6571 (1983).
2. J.A. McCammon, B.R. Gelin, M. Karplus, and P.G. Wolynes, "The hinge-bending mode in lysozyme," *Nature* **262**, 325 (1976).
3. A. Kidera and N. Go, "Refinement of protein dynamic structure: normal mode refinement," *Proc. Natl Acad. Sci. USA* **87**, 3718 (1990).
4. D. Ming, Y. Kong, M.A. Lambert, Z. Huang, and J. Ma, "How to describe protein motion without amino acid sequence and atomic coordinates," *Proc. Natl Acad. Sci. USA* **99**, 8620 (2002).
5. G. Li and Q. Cui, "A coarse-grained normal mode approach for macromolecules: an efficient implementation and application to Ca^{2+}-ATPase," *Biophys. J.* **83**, 2457 (2002).
6. F. Tama, M. Valle, J. Frank, and C.L. Brooks III, "Dynamic reorganization of the functionally active ribosome explored by normal mode analysis and cryo-electron microscopy," *Proc. Natl Acad. Sci. USA* **100**, 9319 (2003).
7. Y. Mizutani and T. Kitagawa, "Direct observation of cooling of heme upon photodissociation of carbonmonoxy myoglobin," *Science* **278**, 443 (1997); "Ultrafast structural relaxation of myoglobin following photodissociation of carbon monoxide probed by time-resolved resonance Raman spectroscopy," *J. Phys. Chem. B* **105**,

10992 (2001); M.D. Fayer, "Fast protein dynamics probed with infrared vibrational echo experiments," *Ann. Rev. Phys. Chem.* **52**, 315 (2001); X. Ye, A. Demidov, and P.M. Champion, "Measurements of the photodissociation quantum yields of MbNO and MbO_2 and the vibrational relaxation of the six-coordinate heme species," *J. Am. Chem. Soc.* **124**, 5914 (2002); F. Rosca, A.T.N. Kumar, D. Ionascu, X. Ye, A.A. Demidov, T. Sjodin, D. Wharton, D. Barrick, S.G. Sligar, T. Yonetani, and P.M. Champion, "Investigations of Anharmonic Low-Frequency Oscillations in Heme Proteins," *J. Phys. Chem. A* **106**, 3540 (2002).

8. B.J. Berne, M. Borkovec, and J.E. Straub, "Classical and modern methods in reaction rate theory," *J. Phys. Chem.* **92**, 3711 (1988); J.I. Steinfeld, J.E. Francisco, and W.L. Hase, *Chemical Kinetics and Dynamics*, Prentice-Hall, New York (1989); A. Stuchebrukhov, S. Ionov, and V. Letokhov, "IR spectra of highly vibrationally excited large polyatomic molecules and intramolecular relaxation," *J. Phys. Chem.* **93**, 5357 (1989); T. Uzer, "Theories of intramolecular vibrational energy transfer," *Phys. Rep.* **199**, 73 (1991).
9. D.E. Logan and P.G. Wolynes, "Quantum localization and energy flow in many-dimensional Fermi resonant systems," *J. Chem. Phys.* **93**, 4994 (1990); S.A. Schofield and P.G. Wolynes, "A scaling perspective on quantum energy flow in molecules," *J. Chem. Phys.* **98**, 1123 (1993); S.A. Schofield, P.G. Wolynes, and R.E. Wyatt, "Computational study of many-dimensional quantum energy flow: from action diffusion to localization," *Phys. Rev. Lett.* **74**, 3720 (1995); S.A. Schofield and P.G. Wolynes, "Rate theory and quantum energy flow in molecules: modeling the effects of anisotropic diffusion and dephasing," *J. Phys. Chem.* **99**, 2753 (1995); D.M. Leitner and P.G. Wolynes, "Vibrational mixing and energy flow in polyatomics: quantitative prediction using local random matrix theory," *J. Phys. Chem. A* **101**, 541 (1997).
10. D.E. Sagnella and J.E. Straub, "A study of vibrational relaxation of B-state carbon monoxide in the heme pocket of photolyzed carboxymyoglobin," *Biophys. J.* **77**, 70 (1999).
11. L. Bu and J.E. Straub, "Vibrational frequency shifts and relaxation rates for a selected vibrational mode in cytochrome c," *Biophys. J.* **85**, 1429 (2003).
12. J.L. Skinner and K. Park, "Calculating vibrational energy relaxation rates from classical molecular dynamics simulations: quantum correction factors for processes involving vibration-vibration energy transfer," *J. Phys. Chem. B* **105**, 6716 (2001).
13. H. Fujisaki, L. Bu, and J.E. Straub, *Adv. Chem. Phys.* B **130**, 179 (2005); e-print q-bio.BM/0403019.
14. D.M. Leitner, "Vibrational energy transfer in helices," *Phys. Rev. Lett.* **87**, 188102 (2001); X. Yu and D.M. Leitner, "Vibrational energy transfer and heat conduction in a protein," *J. Phys. Chem. B* **107**, 1698 (2003).
15. D.M. Leitner, private communication.
16. K. Moritsugu, O. Miyashita, and A. Kidera, "Vibrational energy transfer in a protein molecule," *Phys. Rev. Lett.* **85**, 3970 (2000); "Temperature dependence of vibrational energy transfer in a protein molecule," *J. Phys. Chem. B* **107**, 3309 (2003).
17. D. Keilin, *The History of Cell Respirations and Cytochrome*, Cambridge University Press, Cambridge (1966); R.E. Dickerson, "Cytochrome c and the evolution of energy metabolism," *Sci. Am.* **242**, 136 (1980); G.W. Pettigrew and G.R. Moore, *Cytochromes c: Evolutionary, Structural, and Physiochemical Aspects*, Springer-Verlag, Berlin (1990).

18. S.H. Northrup, M.P. Pear, J.A. McCammon, and M. Karplus, "Molecular dynamics of ferrocytochrome c," *Nature* **286**, 304 (1980); C.F. Wong, C. Zheng, J. Shen, J.A. McCammon, and P.G. Wolynes, "Cytochrome c: a molecular proving ground for computer simulations," *J. Phys. Chem.* **97**, 3100 (1993); A.E. Carcía and G. Hummer, "Conformational dynamics of cytochrome c: correlation to hydrogen exchange," *Proteins: Struct. Funct. Genet.* **36**, 175 (1999); A.E. Cardenas and R. Elber, "Kinetics of cytochrome c folding: atomically detailed simulations," *Proteins: Struct. Funct. Genet.* **51**, 245 (2003); X. Yu and D.M. Leitner, "Anomalous diffusion of vibrational energy in proteins," *J. Chem. Phys.* **119**, 12673 (2003).
19. J.K. Chin, R. Jimenez, and F. Romesberg, "Direct observation of protein vibrations by selective incorporation of spectroscopically observable carbon-deuterium bonds in cytochrome c," *J. Am. Chem. Soc.* **123**, 2426 (2001); "Protein dynamics and cytochrome c: correlation between ligand vibrations and redox activity," *J. Am. Chem. Soc.* **124**, 1846 (2002).
20. J.S. Bader and B.J. Berne, "Quantum and classical relaxation rates from classical simulations," *J. Chem. Phys.* **100**, 8359 (1994).
21. B.R. Brooks, R.E. Bruccoleri, B.D. Olafson, D.J. States, S. Swaminathan, and M. Karplus, "CHARMM: a program for macromolecular energy, minimization, and dynamics calculations," *J. Comput. Chem.* **4**, 187 (1983); A.D. MacKerell, Jr., B. Brooks, C.L. Brooks III, L. Nilsson, B. Roux, Y. Won, and M. Karplus, "CHARMM: the energy function and its parameterization with an overview of the program," in *The Encyclopedia of Computational Chemistry*, vol 1, P.v.R. Schleyer et al., editors, John Wiley & Sons: Chichester (1998), p. 271.
22. R. Kubo, M. Toda, and N. Hashitsume, *Statistical Physics II, Nonequilibrium Statistical Mechanics*, Springer-Verlag, Berlin (1991).
23. M. Shiga and S. Okazaki, "An influence functional theory of multiphonon processes in molecular vibrational energy relaxation," *J. Chem. Phys.* **109**, 3542 (1998); "Molecular dynamics study of vibrational energy relaxation of CN^- in H_2O and D_2O solutions: an application of path integral influence functional theory to multiphonon processes," *J. Chem. Phys.* **111**, 5390 (1999).
24. A.A. Maradudin and A.E. Fein, "Scattering of neutrons by an anharmonic crystal," *Phys. Rev.* **128**, 2589 (1962).
25. V.M. Kenkre, A. Tokmakoff, and M.D. Fayer, "Theory of vibrational relaxation of polyatomic molecules in liquids," *J. Chem. Phys.* **101**, 10618 (1994).
26. P. Hamm, M. Lim, and R.M. Hochstrasser, "Structure of the amide I band of peptides measured by femtosecond nonlinear-infrared spectroscopy," *J. Phys. Chem. B* **102**, 6123 (1998).
27. R. Rey and J.T. Hynes, "Vibrational energy relaxation of HOD in liquid D_2O," *J. Chem. Phys.* **104**, 2356 (1996).
28. R. Rey and J.T. Hynes, "Vibrational phase and energy relaxation of CN^- in water," *J. Chem. Phys.* **108**, 142 (1998).
29. S. Okazaki, private communication.
30. T. Mikami, M. Shiga and S. Okazaki, "Quantum effect of solvent on molecular vibrational energy relaxation of solute based upon path integral influence functional theory," *J. Chem. Phys.* **115**, 9797 (2001).
31. R.B. Gerber, G.M. Chaban, S.K. Gregurick, and B. Brauer, "Vibrational spectroscopy and the development of new force fields for biological molecules," *Biopolymers*, **68**, 370 (2003).
32. B. Madan, T. Keyes, and G. Seeley, "Normal mode analysis of the velocity correlation function in supercooled liquids," *J. Chem. Phys.* **94**, 6762 (1991).

33. J. Cao and G.A. Voth, "A theory for time correlation functions in liquids," *J. Chem. Phys.* **103**, 4211 (1995).
34. A.A. Stuchebrukhov and R.A. Marcus, "Theoretical study of intramolecular vibrational relaxation of acetylenic CH vibration for $v = 1$ and 2 in large polyatomic molecules $(CX_3)_3YCCH$, where X = H or D and Y = C or Si," *J. Chem. Phys.* **98**, 6044 (1993); H.J. Bakker, "Vibrational relaxation in the condensed phase", *J. Chem. Phys.* **121**, 10088 (2004).
35. P.H. Nguyen and G. Stock, "Nonequilibrium molecular-dynamics study of the vibrational energy relaxation of peptides in water," *J. Chem. Phys.* **119**, 11350 (2003).
36. R.B. Gerber, V. Buch, and M.A. Ratner, "Time-dependent self-consistent field approximation for intramolecular energy transfer. I. Formulation and application to dissociation of van der Waals molecules," *J. Chem. Phys.* **77**, 3022 (1982); A. Roitberg, R.B. Gerber, R. Elber, and M.A. Ratner, "Anharmonic wave functions of proteins: quantum self-consistent field calculations of BPTI," *Science*, **268,** 1319 (1995); S.K. Gregurick, E. Fredj, R. Elber, and R.B. Gerber, "Vibrational spectroscopy of peptides and peptide-water complexes: anharmonic coupled-mode calculations," *J. Phys. Chem. B* **101**, 8595 (1997); Z. Bihary, R.B. Gerber, and V.A. Apkarian, "Vibrational self-consistent field approach to anharmonic spectroscopy of molecules in solids: application to iodine in argon matrix," *J. Chem. Phys.* **115**, 2695 (2001). For a review of the VSCF methods, see P. Jungwirth and R.B. Gerber, "Quantum molecular dynamics of ultrafast processes in large polyatomic systems," *Chem. Rev.* **99**, 1583 (1999).
37. T. Terashima, M. Shiga, and S. Okazaki, "A mixed quantum-classical molecular dynamics study of vibrational relaxation of a molecule in solution," *J. Chem. Phys.* **114**, 5663 (2001).
38. Q. Shi and E. Geva, "Semiclassical theory of vibrational energy relaxation in the condensed phase," *J. Phys. Chem.* A **107**, 9059 (2003); "Vibrational energy relaxation in liquid oxygen from a semiclassical molecular dynamics simulation," *J. Phys. Chem. A* **107**, 9070 (2003); "On the calculation of vibrational energy relaxation rate constants from centroid molecular dynamics simulations," *J. Chem. Phys.* **119**, 9030 (2003).
39. H. Kim and P.J. Rossky, "Evaluation of quantum correlation functions from classical data," *J. Phys. Chem. B* **106**, 8240 (2002); J.A. Poulsen, G. Nyman, and P.J. Rossky, "Practical evaluation of condensed phase quantum correlation functions: a Feynman-Kleinert variational linearized path integral method," *J. Chem. Phys.* **119**, 12179 (2003).
40. S. Mukamel and D. Abramavicius, "Many-body approaches for simulating coherent nonlinear spectroscopies of electronic and vibrational excitons," *Chem. Rev.* **104**, 2073 (2004).
41. T. Kato and Y. Tanimura, "Multi-dimensional vibrational spectroscopy measured from different phase-matching conditions," *Chem. Phys. Lett.* **341**, 329 (2001); K. Okumura and Y. Tanimura, "Sensitivity of two-dimensional fifth-order Raman response to the mechanism of vibrational mode-mode coupling in liquid molecules," *Chem. Phys. Lett.* **278**, 175 (1997).